

published in Nucl.
ch Facilities at the
etism: Order and
ram for Scientific



lumblot, J. Kulda,
hysica B 241-243

Otten, R. Surkau,
t, Schearer, Nucl.

A. Meyerhoff, P.J.
hearer, R. Surkau,

nann, W. Heil, D.
tten, D. Rohe, K.
Trautmann, Nucl.

27 May 1999

Physics Letters B 455 (1999) 69-76

PHYSICS LETTERS B

Observation of large change of ${}^7\text{Be}$ decay rate in Au and Al_2O_3 and its implications

A. Ray ^a, P. Das ^a, S.K. Saha ^b, S.K. Das ^b, B. Sethi ^c, A. Mookerjee ^d,
C. Basu Chaudhuri ^d, G. Pari ^d

^a Variable Energy Cyclotron Centre, 1 / AF, Bidhannagar, Calcutta-700064, India

^b Radiochemistry Division, Variable Energy Cyclotron Centre, 1 / AF, Bidhannagar, Calcutta-700064, India

^c Saha Institute of Nuclear Physics, 1 / AF, Bidhannagar, Calcutta-700064, India

^d S.N. Bose National Centre for Basic Sciences, 3 / JD, Bidhannagar, Calcutta-700091, India

Received 14 December 1998; received in revised form 8 March 1999

Editor: R.H. Siemssen

Abstract

We find from our measurements that the decay rate of ${}^7\text{Be}$ implanted in Au is lower than that implanted in Al_2O_3 by a relatively large amount ($0.72 \pm 0.07\%$). This result and others have been analyzed quantitatively using the linear muffin-tin orbital (LMTO) method and Hartree's calculations. Our results are important for accurately extracting the nuclear matrix element of the astrophysically significant ${}^7\text{Be} + e^- \rightarrow {}^7\text{Li} + \nu$ reaction. © 1999 Elsevier Science B.V. All rights reserved.

PACS: 23.40; 26.65

The study of the change of nuclear decay rate in different environments has fundamental significance, as well as applications in nuclear physics, the solar neutrino problem and condensed matter physics. Among the different types of nuclear decay, electron capture by the nucleus is most susceptible to the surrounding environment. Since the surrounding environment can usually only change the configuration of the valence electrons, the effect of the environment will be most prominent on the electron capture rate of ${}^7\text{Be}$, which is the lightest radioactive nucleus that decays by electron capture. The decay rate of ${}^7\text{Be}$ changes slightly when ${}^7\text{Be}$ forms a chemical compound. Such changes [1-4] of decay rates have been measured for many chemical compounds of ${}^7\text{Be}$ and a maximum change of up to $\approx 0.2\%$ has been observed.

Hensley et al. [5] applied a high pressure of up to 270 kilobars to ${}^7\text{BeO}$ and found that the decay rate increased by 0.59%. However, nobody has so far reported seeing such a large change ($\geq 0.5\%$) of decay rate of either implanted ${}^7\text{Be}$ or any of its compounds without applying very high external pressure. We think that if ${}^7\text{Be}$ is implanted in a medium having high electron affinity, such as gold, then beryllium should lose a significant fraction of its 2s electrons as a result of its interaction with nearby gold atoms. It is interesting to study the change in decay rate of ${}^7\text{Be}$ embedded in gold compared to that of ${}^7\text{Be}$ implanted in an insulator such as Al_2O_3 , where the tendency to lose electrons from the 2s orbit of beryllium atom is expected to be much lower. Apart from a general interest in this kind of study, the result of such a measurement is

interesting in astrophysics as well as condensed matter physics. A quantitative understanding of the results of our experiment will enable us to extract accurately the nuclear matrix element of the ${}^7\text{Be} + e^- \rightarrow {}^7\text{Li} + \nu$ reaction which is used to calculate the neutrino emission rate of the sun. These results could also be used to measure the effective electron affinity of a solid medium with respect to beryllium.

We report here our measurement of the difference in the decay rate of ${}^7\text{Be}$ implanted in a gold metal foil and a pellet of Al_2O_3 . ${}^7\text{Be}$ nuclei were produced by bombarding a $250 \mu\text{g}/\text{cm}^2$ -thick foil of lithium fluoride with a 7 MeV proton beam from the Variable Energy Cyclotron Centre, Calcutta. The average proton beam current was $1 \mu\text{A}$ and the lithium fluoride foil was bombarded for 36 h. ${}^7\text{Be}$ nuclei thus produced via the reaction ${}^7\text{Li}(p,n){}^7\text{Be}$ with recoil energy ≈ 3 MeV in the forward direction were implanted in a catcher foil placed behind the target. We used a gold foil and an Al_2O_3 pellet as catchers in which the ranges of 3 MeV ${}^7\text{Be}$ nuclei are $\approx 1.8 \mu\text{m}$ and $2 \mu\text{m}$, respectively. As a result of such implantations, the ${}^7\text{Be}$ atoms were expected to be randomly positioned in the interstitial lattice space of Au and Al_2O_3 . TRIM code calculations [6] indicate that the number of vacancies per Ångström produced in Au and Al_2O_3 lattices by the implanted ${}^7\text{Be}$ atoms is at most only $\approx 0.1\%$ of the number of host atoms per Ångström. The 7 MeV proton beam used for our irradiation work is expected to produce negligible damages in the lattice sites where 3 MeV ${}^7\text{Be}$ ions would stop. These defects do not therefore affect significantly the surrounding environment of the ${}^7\text{Be}$ atoms implanted in Au and Al_2O_3 media. We have ignored the presence of such defects in our considerations.

Following electron capture, a ${}^7\text{Be}$ nucleus has a 10.4% probability of populating the first excited state of ${}^7\text{Li}$ which decays subsequently to its ground state, emitting a 478-keV gamma-ray photon. We measured the difference in the decay rates of ${}^7\text{Be}$ in Au and Al_2O_3 by simultaneously counting the two sources placed 4 m apart. Each source was surrounded properly by at least 10 cm of lead shielding. The irradiated Au foil and Al_2O_3 powder were put in sealed plastic packets and mounted carefully in front of the HPGe detectors. Two HPGe detectors (having an energy resolution of about 2 keV at 1.33

MeV) were used to count 478-keV gamma-ray photons emitted from these two sources. After the irradiation, we waited for 40 days before starting our counting so that all the short-lived isotopes have decayed. A method of differential measurement, as described below was used to measure the small difference in decay rates between the two sources.

Let A_{Au} and A_{AlO} denote the numbers of 478-keV γ -ray photons measured by the corresponding detectors (placed in front of the ${}^7\text{Be}$ -implanted Au and Al_2O_3 sources respectively) within a time period of t to $(t+1)$ days. Let A_{Au}^0 and A_{AlO}^0 be the numbers of 478-keV γ -ray photons detected by the corresponding detectors within the time period from $t=0$ to $t=1$ days. Let λ_{Au} and λ_{AlO} be the decay rates of the ${}^7\text{Be}$ nuclei implanted in Au and Al_2O_3 sources respectively $\lambda_{\text{AlO}} = \lambda_{\text{Au}} + \Delta\lambda$. Then

$$\begin{aligned} & (A_{\text{Au}} - A_{\text{AlO}})\exp(\lambda_{\text{Au}}t) \\ &= (A_{\text{AlO}}^0 \Delta\lambda)t + (A_{\text{Au}}^0 - A_{\text{AlO}}^0) \end{aligned} \quad (1)$$

The shielding around each source was adequate and there was no observable cross-talk between the two detectors. The distance of each source from the corresponding HPGe detector was adjusted carefully to make the single counting rates of two HPGe detectors equal to within 0.3%. Therefore, the pile-up effects of the two detectors were about the same. The integral counting rate of each detector was initially about 850 counts/s and the live times for Au and Al_2O_3 systems were 97.5% and 95.7%, respectively, because the discriminator levels were set slightly differently in the two cases. The lifetimes of the counting systems increased with time as the count rates dropped and the data was corrected appropriately for this factor. The single scalar counts and HPGe spectra were acquired for successive intervals of 24 h duration and then written on a computer disk. This was followed by an automatic reset of the scalars, the erasure of the spectra from the spectrum buffer and the start of data collection for the next 24-h interval.

In Fig. 1, we show typical HPGe γ -ray spectra from both sources, (a) ${}^7\text{Be}$ implanted in Al_2O_3 and (b) ${}^7\text{Be}$ implanted in Au. We find, from this figure, that the integrated background counts under the 478 keV line are less than 0.1% of the total integrated counts under the 478 keV peak. We also noted a

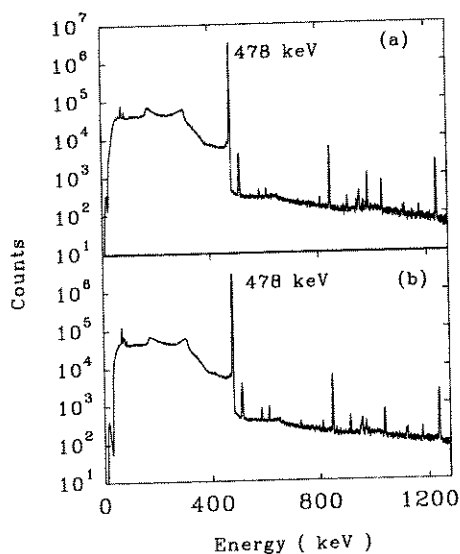


Fig. 1. γ -ray spectra from the decay of ${}^7\text{Be}$ implanted in (a) an Al_2O_3 pellet and (b) Au foil.

(1)

adequate and
ween the two
ce from the
sted carefully
f two HPGe
e, the pile-up
he same. The
was initially
s for Au and
respectively,
set slightly
times of the
as the count
ted appropri-
r counts and
sive intervals
computer disk.
reset of the
the spectrum
for the next

γ -ray spectra
in Al_2O_3 and
m figure,
under the 478
total integrated
also noted a

number of very low intensity background- and impurity-lines in both Fig. 1(a) and Fig. 1(b). A careful study of these low intensity background lines showed that many of them (511 keV, 583 keV, 609 keV, 727 keV, 911 keV, 969 keV, 1120 keV) were the standard background gamma lines which came from the naturally present long-lived radioactive isotopes and were seen in the room background spectra also. In addition, we saw 847 keV, 978 keV, 1038 keV, 1175 keV, 1238 keV and 811 keV gamma-ray lines which indicated the presence of ${}^{56}\text{Co}$ (half-life = 78.8 days) and ${}^{58}\text{Co}$ (half-life = 70.8 days) in our samples. We think that there was very small amount of iron contamination in our samples and ${}^{56}\text{Co}$ and ${}^{58}\text{Co}$ were produced via (p,n) reactions. It looks as though the iron was the main contaminant in our samples and that it was present at about 0.2%. We also saw indications of the presence of both a very small amount of ${}^{65}\text{Zn}$ in both of the samples and that of ${}^{48}\text{V}$ in Al_2O_3 . These isotopes could be produced from ${}^{65}\text{Cu}$ and ${}^{48}\text{Ti}$ via (p,n) reactions.

Therefore all the gamma-ray lines are well understood and the observed contaminants cannot produce any gamma-ray lines in the region of 478 keV. In order to check further, we looked up a gamma-ray catalog [7] and searched for the isotopes which emit

gamma rays in the region (478 ± 4) keV and satisfy the following required conditions: (i) a reasonably long half-life (at least of the order of a few days or longer) in order to survive after a 40-day waiting time, (ii) the possibility of producing the isotope using a 7 MeV proton beam on a stable nucleus; and (iii) the observation of the accompanying gamma-ray lines. We did not find any such isotope satisfying the required conditions and so we can rule out the possibility of any background peaks under the 478 keV line.

The counts under the 478 keV peaks were determined from each day's spectra and corrected by the corresponding computer lifetime correction factor. The integrated number of counts under the 478 keV peak was of the order of 10^7 counts. The differential measurement between the activities of the two sources was performed for 65 days. Then, the position of the sources was interchanged and the differential measurement was performed again for 83 days. Such an interchange of source positions was done so that any systematic error would be cancelled out when an average of the two measurements would be taken. Fig. 2 shows plots of $(A_{\text{Au}} - A_{\text{AlO}})\exp(\lambda_{\text{Au}}t)$ versus t for the two interchanged positions and the values of $(A_{\text{AlO}}^0 \Delta\lambda)$, determined from their slopes in both cases. The values of A_{AlO}^0 were determined from the plots of $\ln(A_{\text{AlO}})$ versus t . The value of A_{AlO}^0 depends on the initial number of ${}^7\text{Be}$ nuclei at the $t=0$ instant, the decay rate, the branching ratio for the 478 keV γ -ray photons, the detection efficiencies and the counting time. When the sources were interchanged and the counting was restarted, a new $t=0$ instant was defined and the new value of A_{AlO}^0 was smaller than the previous value as the number of ${}^7\text{Be}$ nuclei had decreased in the intervening time. Using Eq. (1), the corresponding values of $\Delta\lambda$ were then determined. We obtained values of $\frac{\Delta\lambda}{\lambda} = (0.00705 \pm 0.00072)$ from Fig. 2(a) and $\frac{\Delta\lambda}{\lambda} = (0.0078 \pm 0.0016)$ from Fig. 2(b). The linear correlation coefficients in the two cases were 0.84 and 0.81 respectively. The weighted average from the two sets of data points was $\frac{\Delta\lambda}{\lambda} = (0.0072 \pm 0.0007)$. The uncertainty given here is statistical only.

Finally, we removed both the sources and cut the Au foil in which ${}^7\text{Be}$ was implanted into two equal halves. We placed then the two Au foils in front of two HPGe detectors and performed a differential

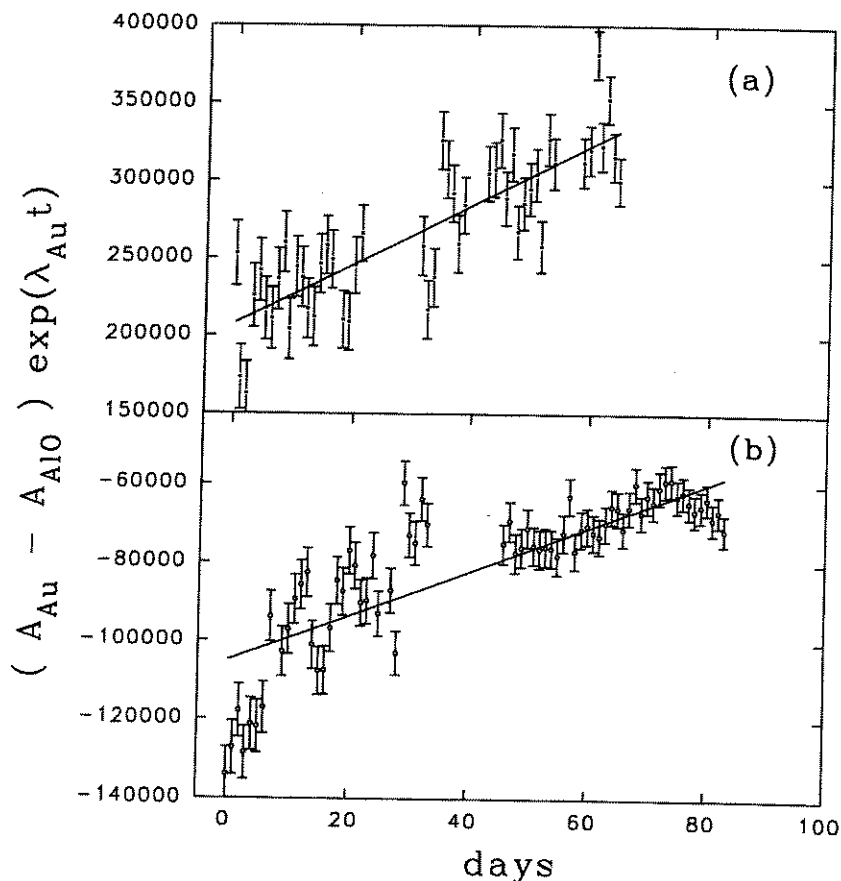


Fig. 2. (a) Plot of $(A_{\text{Au}} - A_{\text{AlO}}) \exp(\lambda_{\text{Au}} t)$ versus time and (b) the same plot after interchanging the positions of the sources.

measurement of their decay rates for 40 days. In Fig. 3, we show a plot of $(A_{\text{Au1}} - A_{\text{Au2}}) \exp(\lambda_{\text{Au}} t)$ versus t , where A_{Au1} , A_{Au2} are activities of the two pieces of Au foil in which ${}^7\text{Be}$ nuclei were implanted. We found a horizontal line consistent with $\Delta\lambda = 0$, as expected in this case. From Fig. 3, we concluded that the systematic error in our result was less than 0.2%. We also studied whether our result depends on how the peak areas under the 478 keV lines were determined. After studying different methods of background subtraction and peak-area determination, we finally concluded that our results and the quality of linear fits in Fig. 2 were essentially independent of the peak area determination method used as long as any reasonable method is used consistently throughout the analysis.

A qualitative understanding of our result can be obtained from the fact that Au has a high electron affinity (2.308 eV) [8]. We expect that Al_2O_3 does not have any significant electron affinity. The electron affinity of beryllium is -0.19 eV [8]. The negative value of electron affinity for beryllium means that there is no bound state of an extra electron to the ground state of the beryllium atom. Therefore, a beryllium atom implanted in Au should lose a larger fraction of its 2s electrons compared to a beryllium atom implanted in Al_2O_3 . As a result, the decay rate of ${}^7\text{Be}$ in Au should be slow compared to that in Al_2O_3 .

In order to get a quantitative understanding of our results, we performed tight-binding linear muffin-tin orbital (TB-LMTO) method [9] calculations and

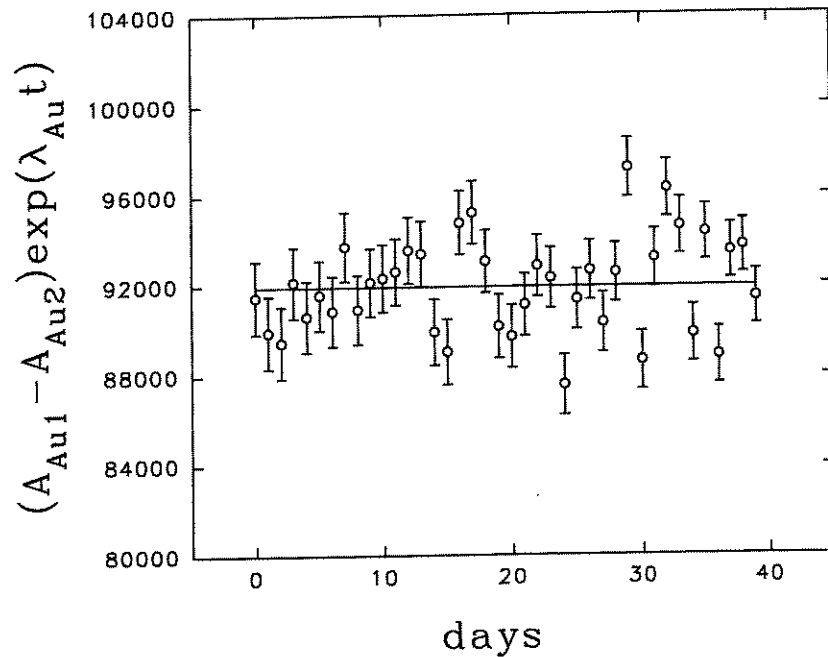


Fig. 3. Plot of $(A_{Au1} - A_{Au2})\exp(\lambda_{Au} t)$ versus time. Both the sources (^7Be in Au) are identical and null result is found.

compared the result of such calculations with our experimental results. In the TB-LMTO method, the interatomic potential is assumed to be of the muffin-tin type and is written as

$$V_{MT}(r) = V_i(r_i) + \sum_R V_R(r_R) \equiv V_0 + \sum_R v_R(r_R) \quad (2)$$

where $V_R(r_R)$ and $v_R(r_R) \equiv V_R(r_R) - V_0$ are spherically symmetric inside a sphere of radius s_R centered at R and vanish outside. $V_i(r_i)$ takes the constant value V_0 (the muffin-tin zero) in the interstitial region and vanishes outside. A beryllium atom is put in the interstitial region and a spherically symmetric potential is considered centered around this atom. This spherical potential also vanishes outside a certain radius. Schrodinger's equation was solved for this problem assuming periodic boundary condition. Atomic muffin-tin orbitals are considered spherical and no deformation due to the overlap of two nearby muffin-tin orbitals has been considered. A detailed theoretical paper on these calculations will be published later [10]. For a given position of the implanted beryllium atom and the assumption of spher-

ical potential, the LMTO method performs a first principle calculation and there is no adjustable free parameter in the calculation. Let Ψ_{total} be the complete electronic wave function and $\Psi_{\text{Be}2s}$ be beryllium 2s state wave function. We calculated the square of the overlap of Ψ_{total} with $\Psi_{\text{Be}2s}$ i.e. $|\langle \Psi_{\text{total}} | \Psi_{\text{Be}2s} \rangle|^2$, which represents the average number of 2s electrons in a beryllium atom when it is implanted in a material. We find that this average number of beryllium 2s electrons depended on the position of beryllium atom in the interstitial region. In the case of implantation in a gold foil, as a beryllium atom comes closer to a gold atom, it loses more electrons from 2s state. When we placed a beryllium atom at the body center position of gold lattice, then we found, from our calculations, that $|\langle \Psi_{\text{total}} | \Psi_{\text{Be}2s} \rangle|^2 = 0.67$. When we shifted the beryllium atom from this symmetric position in any direction, then the beryllium atom rapidly lost more and more 2s electrons. Since beryllium atoms are implanted by irradiation, they will be randomly positioned in the interstitial space. The beryllium atoms cannot come too close to a gold atom because of Coulomb repulsion. The ratio of overlap volume

ie sources.

ir result can be a high electron at Al_2O_3 does inity. The elec- 9 eV [8]. The for beryllium te of an extra beryllium atom. ed in Au should ns compared to D_3 . As a result, l be slow com-

rstanding of our inear muffin-tin calculations and

between the nearest atoms to their total volumes enters into the LMTO calculation as a perturbation term. We considered an overlap of nearest atomic volumes of up to 10%. In our LMTO code, we moved the implanted beryllium atom around to various interstitial positions so that the maximum overlap was within 10% and then took a weighted average. From the symmetric position at the center of the face centered cubic (FCC) lattice, if the beryllium atom was shifted straight down, then we could shift it only slightly more than one tenth of the lattice length (4.08 Å). However when we shifted beryllium atom along the diagonal direction, we could shift it up to three tenths of the lattice length. We took an average over 15 different positions of beryllium atom in the interstitial space (the symmetric position in the center of FCC lattice and 14 shifted positions in all directions around the symmetric position) and found that the average number of 2s electrons of a beryllium atom implanted in a gold foil was 0.416. When the overlap of the atomic volumes is reduced by 10%, then this number increased by about 10%. The remaining electrons of beryllium atom go to the p-state and d-state of the ^7Be atom and do not contribute to the electron density at the atomic nucleus ($r = 0$).

When we placed a beryllium atom in Al_2O_3 medium, then $|\langle \Psi_{\text{total}} | \Psi_{\text{Be}2s} \rangle|^2 = 0.864$. This number for Al_2O_3 was relatively insensitive to the position of the beryllium atom in the interstitial region. Thus we finally arrived at the conclusion that the beryllium atom implanted in gold will have on the average 0.448 number of 2s electrons less compared to that of a beryllium atom implanted in Al_2O_3 . We know from Hartree's calculations [11] that the square of the beryllium 2s electronic state wave function (2 electrons) to that of the 1s state wave function at the nucleus ($r = 0$) is 3.31%. The exchange and overlap corrections change the L/K vacancy ratio in the ^7Li atom, but their effect on the total decay rate of ^7Be is less than 0.1% and we neglected them. The effect of 0.448 beryllium 2s electrons on the ^7Be decay rate was 0.74%. According to this model, the decay rate of ^7Be implanted in gold should therefore be slowed down by 0.74% compared to the decay rate of ^7Be in Al_2O_3 . Our theoretical estimate was in good agreement with our experimental observation of $\frac{\Delta\lambda}{\lambda} = (0.0072 \pm 0.0007)$.

Let us now compare our theoretical calculations with other available experimental results. We find from the experimental work of Jaeger et al. [12] and Lagoutine et al. [13] that the decay rate of ^7Be in aluminum is slower by $0.1 \pm 0.2\%$ compared to that in lithium fluoride, whereas our calculations show that the corresponding slow down should be 0.08%. The reason for such small change in the decay rate of ^7Be when implanted in aluminum is the much lower electron affinity of aluminum (0.441 eV) [8]. Very recently, Norman et al. [14] reported measurements of half-lives of ^7Be in gold and tantalum. They used a ^7Li beam on a hydrogen target and the recoiled ^7Be ions were implanted on a catcher foil placed behind the target [14]. Their results show that the decay rate of ^7Be in gold is slower than that in tantalum by $(0.22 \pm 0.13)\%$, whereas our calculations show that the corresponding slow down of decay rate in gold should be 0.3%. Although the electron affinity of tantalum is small (0.322 eV) [8], tantalum has a small body-centered lattice structure. So the distance between the implanted beryllium atom and nearest tantalum atom is therefore small, thus increasing tantalum's effective electron affinity which is determined by the atomic electron affinity and lattice geometry. The decay rate of ^7Be in tantalum is thus comparatively slower and the difference in decay rate in comparison with gold is smaller. Comparisons of Norman et al.'s results [14] with Refs. [13,12] show that the decay rate of ^7Be in gold is slower than those in aluminum and lithium fluoride by $(0.27 \pm 0.15)\%$ and $(0.36 \pm 0.15)\%$ respectively. Our calculations show that the decay rates in gold should be slower than those in aluminum and lithium fluoride by 0.45% and 0.53% respectively. Norman et al. [14] thus apparently found a somewhat smaller increase in the half-life of the ^7Be implanted in gold compared to our observations and calculations. Since Norman et al. used heavy ion ^7Li beam for their implantation studies, the radiation damage on gold lattice sites where ^7Be nuclei stop would be much larger [6] (3×10^{-4} vacancies/Ångstrom/ion) than the corresponding damages (1×10^{-5} vacancies/Ångstrom/ion) for our proton irradiation work. The effective electron affinity of gold lattice will be reduced because of such damages and this effect should reduce the half-life of the implanted ^7Be nuclei in gold. Our calculations do not take into

account any lattice damage effects. We therefore conclude that our observations regarding the change of the ${}^7\text{Be}$ decay rate in gold compared to that in Al_2O_3 and other available experimental results are reasonably well understood in terms of the TB-LMTO method and Hartree's calculations.

Let us now discuss the implications of our work for accurately determining the nuclear matrix element of the astrophysically important ${}^7\text{Be} + e^- \rightarrow {}^7\text{Li} + \nu$ reaction. Our observations as well as TB-LMTO calculations show that a ${}^7\text{Be}$ atom loses significant fraction of its 2s electrons when it is placed in gold (average number of 2s electrons = 0.416) or even in Al_2O_3 (average number of 2s electrons = 0.864). Such considerations are important for accurately extracting the nuclear matrix element of astrophysically significant ${}^7\text{Be} + e^- \rightarrow {}^7\text{Li} + \nu$ reaction. Bahcall et al. [15–17] took the ${}^7\text{Be}$ half-life from the work of Segre et al. [1] and Kraushaar et al. [2] and extracted the corresponding nuclear weak-interaction matrix element, assuming that the beryllium atomic wave function was the same as if the beryllium atom was in free space and it had two full 2s electrons. They subsequently used this matrix element to calculate the ${}^7\text{Be}$ decay rate of the sun. Their calculation is generally believed to be accurate within 1–2%. However, both Segre et al. [1] and Kraushaar et al. [2] measured the decay rates of ${}^7\text{Be}$ in natural nonradioactive beryllium metal (${}^9\text{Be}$). In the process of preparing their sample, a mixture of beryllium oxide and zirconium powder was heated under vacuum at 1300°C the beryllium metal distilled away from the zirconium and was collected on a cone shaped cold finger. In this process, ${}^7\text{Be}$ atoms are expected to occupy lattice sites in ${}^9\text{Be}$ lattices. Our TB-LMTO calculations predict that in this situation, the average number of 2s electrons in ${}^7\text{Be}$ would be $|\langle \Psi_{\text{total}} | \Psi_{\text{Be}2s} \rangle|^2 = 0.831$. Based using Hartree's results [11] as discussed earlier, we conclude that the change of decay rate due to the loss of 1.169 number of 2s electrons from ${}^7\text{Be}$ atom would be = 1.9%. Bahcall [16] computed the value of the overlap of electron wave function at the nucleus using the formula

$$A = \frac{1}{4\pi^2} \left[\{g_{1,-1}(0)\}^2 + \{g_{2,-1}(0)\}^2 \right] \quad (3)$$

where $g_{1,-1}(0)$ and $g_{2,-1}(0)$ are the values of 1s and 2s electronic wave functions at the nucleus. Following Hartree's calculations [11], Bahcall [16] took the values of electronic wave functions at the nucleus as (in atomic units) $g_{1,-1}(0) = 14.67$ and $g_{2,-1}(0) = 2.67$ and computed the value of A.

Since, according to our LMTO calculations, the average number of 2s electrons in a beryllium atom occupying a lattice site in beryllium metal is 0.831, in this case, $g_{2,-1}(0)$ should be = 1.72 and consequently, the value of A would decrease by 1.9%, thus increasing the extracted nuclear matrix element of the ${}^7\text{Be} + e^- \rightarrow {}^7\text{Li} + \nu$ reaction by 1.9%. As a result, following Bahcall's arguments [18], the prediction for ${}^8\text{B}$ production in the sun and associated neutrino flux should decrease by 1.9%, slightly reducing the discrepancy between the theory and experiment in the solar neutrino problem. At present, the uncertainty of the predicted ${}^8\text{B}$ solar neutrino flux is more than 10% [18] mainly due to the uncertainty in the measured ${}^7\text{Be}(p,\gamma){}^8\text{B}$ reaction rate. The current generation of ${}^7\text{Be}(p,\gamma){}^8\text{B}$ experiments will probably bring down this uncertainty within 5%. The result of this paper would then be useful for better understanding of the solar interior, solar helioseismological data as well as the neutrino physics using the solar neutrino data from the current-generation experiments.

In summary, we measured a large change in the ${}^7\text{Be}$ decay rate in gold and aluminum oxide and analyzed this result and other available experimental results using the linear muffin-tin orbital method and Hartree's calculations. We found that a combination of atomic electron affinity and geometry of the lattice determined an effective electron affinity of the medium which is responsible for the change of the decay rate of the implanted ${}^7\text{Be}$ nuclei in different media. Our results also suggest that the predicted ${}^8\text{B}$ solar neutrino flux should be 1.9% lower than the standard value.

Acknowledgements

We acknowledge useful discussions with Eric Norman (Lawrence Berkeley Laboratory), John Bahcall (Institute of Advanced Study, Princeton University), R. Vandenbosch (University of Washing-

ton) and Ashoke Chatterjee (University of Kalyani, India). We also thank Amitava Roy and Tushar Das (VECC) for helping us with data acquisition system and the cyclotron staff of VECC for the smooth operation of the machine.

References

- [1] E. Segre, C.E. Weigand, *Phys. Rev.* 75 (1949) 39.
- [2] J.J. Kraushaar, E.D. Wilson, K.T. Bainbridge, *Phys. Rev.* 90 (1953) 610.
- [3] H.W. Johlige, D.C. Aumann, H.J. Born, *Phys. Rev.* C2 (1970) 1616.
- [4] G.T. Emery, *Ann. Rev. Nucl. Sci.* 22 (1972) 165.
- [5] W.K. Hensley, W.A. Basset, J.R. Huizenga, *Science* 181 (1973) 1164.
- [6] J.F. Ziegler, J.P. Bierserk, U. Littmark, 'The Stopping and Range in Solids', Pergamon Press, NY, 1985.
- [7] U. Reus, W. Westmeier, I. Warnecke, *Gamma ray Catalog*, GSI-Report, February, 1979.
- [8] *CRC Handbook of Chemistry and Physics*, by R. David (Ed.), Lide, 1994-95.
- [9] O.K. Andersen, O. Jepsen, D. Glotzi, *Highlights of Condensed Matter Theory* (North-Holland, New York), 1985; O.K. Andersen, Z. Pawlowska, O. Jepsen, *Phys. Rev.* B34 (1986) 5253.
- [10] A. Mookerjee et al., to be published.
- [11] D.R. Hartree, W. Hartree, *Proc. Roy. Soc. (London)* A 150 (1935) 9.
- [12] M. Jaeger, S. Wilmes, V. Kojic, G. Staudt, *Phys. Rev.* C54 (1996) 423.
- [13] F. Lagoutine, J.L. Legrani, C. Bac, *International Journal of Applied Radiation and Isotopes* 25 (1975) 131.
- [14] E.B. Norman et al., *Bull. Am. Phys. Soc.* 43 (1998) 1548.
- [15] J.N. Bahcall, *Phys. Rev.* 126 (1962) 1143.
- [16] J.N. Bahcall, *Phys. Rev.* 128 (1962) 1297.
- [17] J.N. Bahcall, Walter F. Huebner, Stephen H. Lubow, Peter D. Parker, Roger K. Ulrich, *Rev. Mod. Phys.* 54 (1982) 767.
- [18] J.N. Bahcall, *Astrophysical Journal* 467 (1996) 475.